CHEMISTRY
AN ASIAN JOURNAL
ACES
FULL PAPER

DOI: 10.1002/asia.201402247

Synthesis, Crystal Structures, Optical Properties, and Photocurrent Response of Heteroacene Derivatives

Tiejun Ren,[a] Jinchong Xiao,*[a] Wenying Wang,[a] Wenya Xu,[b] Sujuan Wang,[a] Xuemin Zhang,[a] Xuefei Wang,*[c] Hua Chen,*[a] Jianwen Zhao,*[b] and Li Jiang[d]

Abstract: Six 5,9,14,18-tetrathiaheptacene derivatives (**1a**–**1f**) were synthesized by using a simple ether–ether exchange reaction and fully characterized. In contrast to the planar conformation usually observed in thiophene-fused benzene systems, single-crystal analysis indicates that 7,16-dipropyl-5,9,14,18-tetrathiaheptacene (**1a**), 7,16-diphenyl-5,9,14,18-tetrathiaheptacene (**1b**), and 7,16-di(4′-chlorophenyl)-5,9,14,18-tetrathiaheptacene (**1c**) adopt chair conformations. The as-formed dihedral angle between anthracene and the terminal benzene units are 137.258, 137.855, and 134.912° for **1a**, **1b**, and **1c**, respectively, which is close to the theoretical optimization results (128° for **1b**). Interestingly, the oxidized product of 7,16-di(trifluoromethylphenyl)-5,9,14,18-tetrathiaheptacene (**1e**) has a saddle shape, which results in the formation of column-shaped units in the single crystal. The substituents on the side phenyl group have less effect on their UV/Vis absorption spectra, but a distinct redshift that accounts for the intramolecular charge transfer can be observed in the emission spectra. The electrochemical measurements show that all compounds present two oxidation waves. The photoswitching behavior based on **1a**–**1f** was further measured and the experimental results suggest that these heteroacene derivatives are promising semiconductor materials for organic electronics.

Keywords: acene · conformation analysis · optical properties · semiconductors · X-ray diffraction

Introduction

Flexible optoelectronic devices based on organic semiconductors have been increasingly acknowledged in recent decades because these π-conjugated molecules can be easily decorated with different substituents that present interesting properties. They can be employed in artificial light-harvesting systems, organic field-effect transistors (OFETs), light-emitting diodes (LEDs), lasers, photovoltaic cells, photoresponse materials, and biological fluorescence probes.[1–22] Thus there are currently many scientific research groups in continuous pursuit of delicate molecular design and rational preparation of organic semiconductors with high optoelectronic performance.

Acene is a type of carbon material with a linear structure of fused benzene rings that was first introduced by Clar[23] and represents a fascinating class of organic conjugated molecules. These one-dimensional molecules were considered to not only have similar properties to graphene and conducting polymers, but also provide more information about structure–property relationships. The physical properties have attracted much attention from both theorists and synthetic researchers. For example, Kivelson and Chapman speculated that large acenes might show superconductivity at high temperature based on theoretical calculations.[24] Moreover, studies by Houk et al.[25] and Bendikov et al.[26,27] showed that the large acene has a biradical state. In addition, tetracene, pentacene, hexacene, and their derivatives have been employed in organic electronics that exhibits high electroluminescence effect and charge-carrier ability.[28–30] To date, some larger acenes, such as heptacenes and nonacenes, have been isolated but studies of their performance are scarce due to difficulties with scale-up, purification, easy oxidation in air, and photosensitivity. In particular, this type of compound usually has a higher HOMO level, which leads to high electronegativity, that is, poor stability in air. For exam-

[a] Dr. T. Ren, Prof. J. Xiao, Dr. W. Wang, Dr. S. Wang, Dr. X. Zhang, Prof. H. Chen
College of Chemistry and Environment Science
Key Laboratory of Chemical Biology of Hebei Province
Hebei University
Baoding, 071002 (P.R. China)
E-mail: jcxiaoiccas@gmail.com
hua-todd@hbu.edu.cn

[b] Dr. W. Xu, Prof. J. Zhao
Printable Electronics Research Centre
Suzhou Institute of Nanotech and Nanobionics
Chinese Academy of Sciences
Suzhou 215123 (P.R. China)
E-mail: jwzhao2011@sinano.ac.cn

[c] Prof. X. Wang
School of Chemistry and Chemical Engineering of
University of Chinese Academy of Sciences
Beijing 100049 (P.R. China)
E-mail: wangxf@iccas.ac.cn

[d] Prof. L. Jiang
Beijing National Laboratory for Molecular Sciences
Laboratory of Molecular Nanostructure and Nanotechnology
Institute of Chemistry
Beijing 100190 (P.R. China)

Supporting information for this article is available on the WWW under http://dx.doi.org/10.1002/asia.201402247.

ple, Wudl and co-workers synthesized a stable triisopropylsilylethynyl-decorated heptacene with a nonzero band gap.[31] The groups of Miller, Zhang, and Anthony reported a series of stable arylthio-, phenyl- and fluorine-functionalized nonacenes, the absorption spectra of which were localized in the near-infrared region.[32–34]

To overcome the poor stability in air, the modification of heteroatoms inserted into the building blocks was considered.[35–44] In this way, the isolation and structural characterization of the as-prepared heteroacenes could be carried out easily and the optoelectronic properties also could be optimized through rational molecular design. Moreover, the intermolecular arrangement and stacking in the solid state might be tuned to improve the thermal and chemical stability. At present, the heteroatoms mainly refer to boron, nitrogen, phosphorus, and chalcogen atoms. As with organic semiconductors, the selection of heteroatoms plays an important role in the modification of acene properties. Previously, several heteroatom-modified organic conjugated molecules have been synthesized and opened a path to fascinating applications in organic electronic materials.[45–51] In the case of sulfur atoms incorporated in acenes, Anthony and Takimiya et al., respectively, successively reported the synthesis of a series of thiophene–benzene fused systems, and one of them could exhibit high field-effect mobility of 5 $cm^2 V^{-1} s^{-1}$ in thin-film devices.[28,52] Note that thiophene and benzene rings in these systems are usually in one plane. However, the nonplanar 1,4-dithiine-fused acene derivatives with six-membered rings in the main backbone have been scarcely investigated. Although Lin and Radhakrishnan[53] reported the synthesis of an isomeric mixture of 7,16-diphenyl-5,9,14,18-tetrathiaheptacene, herein we are particularly interested in nonplanar acene, especially the detailed crystal spatial structure, optoelectrical properties, and applications as photocurrent materials.

Herein, we present our fundamental research of the synthesis and characterization of six tetrathiaheptacene derivatives (**1a–1f**) that have chair conformation observed by using single-crystal X-ray analysis (Scheme 1). Additionally, the substituent effect on the optoelectronic properties was also studied in detail. In addition, to investigate photoswitching behavior, photocurrent devices based on compounds **1a–1f** were fabricated and tested.

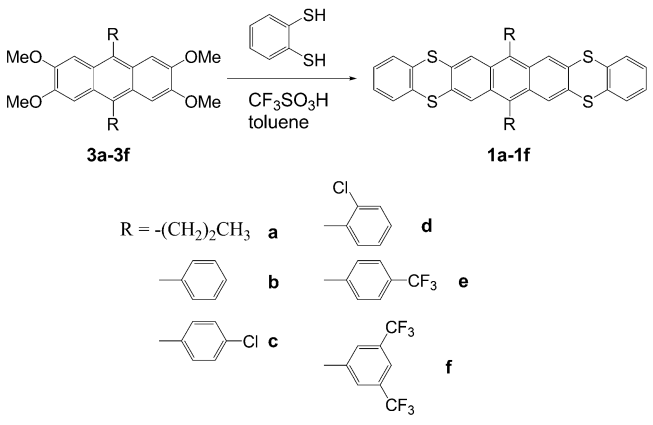

Scheme 1. Synthesis of heteroacene derivatives **1a–1f**.

Results and Discussion

The synthetic routes of compounds **1a–1f** depicted in Scheme 1 and the detailed experimental procedure is presented in the Supporting Information. Alkyl- and aryl-substituted anthracene intermediates **3a–3f** were obtained through condensation of 1,2-dimethoxylbenzene with *n*-butyl aldehyde or aromatic aldehyde catalyzed by sulfuric acid as described earlier.[54] The as-formed intermediates (**3a–3f**) were further treated with 1,2-benzenedithiol (**2**) in the presence of triflic acid in dry toluene through an ether–ether exchange reaction to afford target compounds **1a–1f**.[53] It should be noted that the ether–ether exchange process must be completed in dry solvent, otherwise more by-products were obtained due to the competitive reaction between water and 1,2-benzenedithiol. Moreover, as-prepared compounds **1a–1f** are stable in the solid state under ambient conditions. Note that we could not obtain the ^{13}C NMR spectrum for the 9,10-bis(2-chlorophenyl)-2,3,6,7-tetramethoxyanthracene precursor (**3d**) owing to the instability in $CDCl_3$ solution. In addition, the ^{13}C NMR spectra of compounds **1c–1f** were not obtained because of their poor solubility.

Single-crystal analysis was carried out to evaluate the spatial arrangement. After slow diffusion of methanol into a solution of these derivatives in methylene chloride or chloroform at room temperature, crystals suitable for X-ray analysis of compounds **1a–1c** were obtained. Their topology structures and three-dimensional packing model are shown in Figure 1 and the corresponding crystallographic data are compiled in Table S1 in the Supporting Information. Compounds **1a** and **1c** were observed to have monoclinic crystal systems whereas **1b** has a triclinic unit cell. The unit cell parameters are $a=12.2585(10)$, $b=10.7338(8)$, $c=10.5914(8)$ Å; $\alpha=90$, $\beta=108.302(10)$, $\gamma=90°$ for **1a**; $a=10.518(3)$, $b=11.339(3)$, $c=13.665(3)$ Å; $\alpha=79.850(4)$, $\beta=68.853(4)$, $\gamma=78.721(4)°$ for **1b**; and $a=14.363(2)$, $b=23.342(4)$, $c=10.5722(16)$ Å; $\beta=95.87°$ for **1c**. The four sulfur atoms and the anthracene unit are nearly planar, whereas one terminal phenyl moiety is oriented above the central anthracene plane and the other is bent below this plane. Note that the as-formed dihedral angle between anthracene and the terminal benzene are 137.258, 137.855, and 134.912° for **1a**, **1b**, and **1c**, respectively. The findings suggest that not only can the as-prepared molecules form chair conformations, but also that the *para*-chlorine atoms in the phenyl unit might cause an increase in coplanarity for heteroacene derivatives to a lesser extent. In addition, the pendant phenyl and 4-chlorophenyl units in compounds **1b** and **1c** are nearly orthogonal to anthracene part (80.341° for **1b**, 86.937° for **1c**). In the packing model, the mismatched structures of compounds **1a–1c** displace between the neighboring

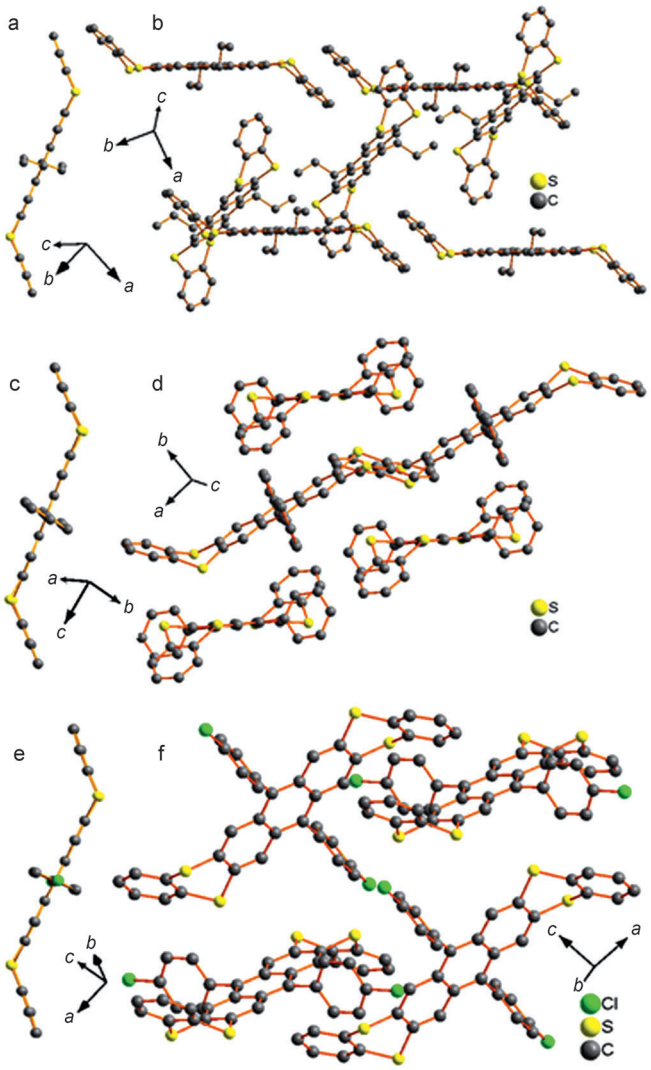

Figure 1. X-ray single crystal structures of a) **1a** and b) the packing model, c) **1b** and d) the packing model, e) **1c** and f) the packing model. Carbon, sulfur and chlorine atoms are shown in gray, yellow, and green, respectively. Hydrogen atoms are omitted for clarity.

molecules, which might result from a steric encumbrance hindrance. Additionally, the neighboring molecules have a long vertical distance, which implies no π–π intermolecular stacking in the crystalline state. Clearly, the as-formed structures could not be beneficial for charge transfer.[55]

As mentioned for **1d** and **1f**, the light-green single crystal is too small to perform X-ray analysis. Interestingly, when methanol was slowly dispersed into a solution of **1e** in chloroform, small green single crystals were also formed in 3 d. ^{1}H NMR spectroscopy and MALDI-TOF spectrometry were used to confirm that the crystals were **1e**. However, we observed that the as-formed light-green prismatic crystals gradually changed to white crystals within one week. On the base of ^{1}H NMR spectroscopy and MALDI-TOF results (Figure S23 in the Supporting Information), we observed that the signals at $\delta = 7.94$, 7.65, 7.56, 7.44, and 7.23 ppm disappeared and a new mass peak with m/z 775.0 was obtained (Figure S24 in the Supporting Information), which provides strong evidence that oxidation of compound **1e** took place and oxidized product **1e-ox** was formed as shown in Scheme 2. The proposed structure of **1e-ox** was further confirmed by using X-ray diffraction (Figure 2). The results indicate that compound **1e-ox** adopts a saddle-shaped molecular structure, in which the oxygen atoms and

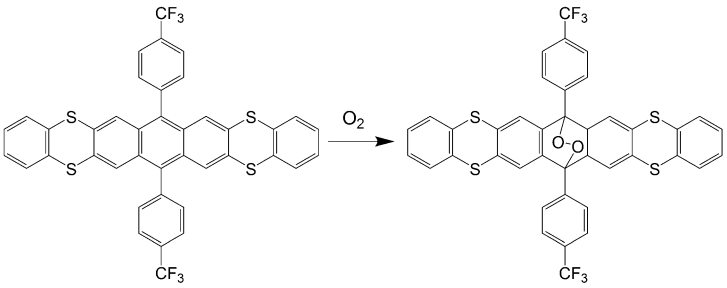

Scheme 2. The oxidation procedure of compound **1e** to **1e-ox**.

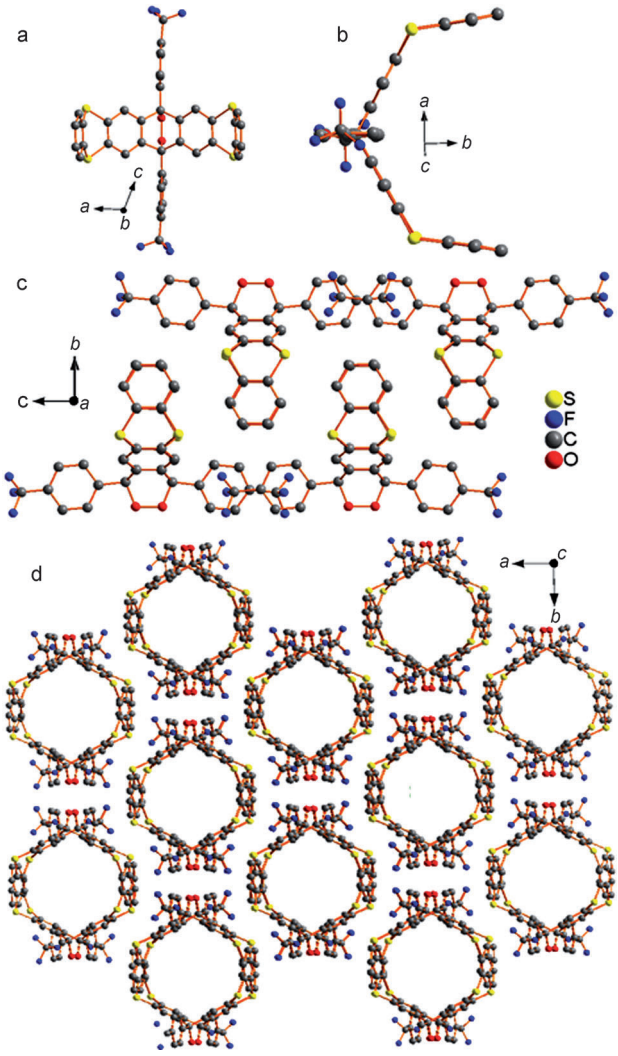

Figure 2. Crystal structure of compound **1e-ox**: a) side view, b) top view, c) side view of packing model, and d) top view of packing model.

peripheral 4-trifluoromethylphenyl unit take a planar geometry and orient perpendicular to central phenyl group in the heteroacene framework (Figure 2a and b). Interestingly, the crystal analysis reveals a cylindrical unit (Figure 2c and d) with a diameter of approximately 10.529 Å, which is close to the van der Waals diameter of a C_{60} molecule (1.1 nm).[56]

CCDC-980773 (**1a**), -980774 (**1b**), -980775 (**1c**), and -980772 (**1e-ox**) contain the supplementary crystallographic data for this paper. These data can be obtained free of charge from The Cambridge Crystallographic Data Centre via www.ccdc.cam.ac.uk/data_request/cif.

The UV/Vis and fluorescence spectra of compounds **1a**–**1f** were investigated in diluted methylene chloride at room temperature. The spectra are shown in Figure 3 and the detailed data are presented in Table S2 in the Supporting Information. Compound **1a** features absorption peaks at $\lambda =$ 437, 410, 389, and 329 nm. In comparison, the spectra of aromatic-substituted derivatives **1b**–**1f** display similar profiles and somewhat blueshifted peaks at $\lambda = 430$, 406, and 384 nm, which are indicative of the weak effect of the peripheral groups. It is interesting to note that the peaks in the range of $\lambda = 370$ to 460 nm looks like fingers, which is a typical characteristic of acene and its derivatives.[31,57–59] When excited at $\lambda = 410$ nm, propyl-decorated compound **1a** exhibits a vibrational structure and maximum peak at $\lambda = 478$ nm with a shoulder band at $\lambda = 450$ nm (Figure 3b). However, with an increase in electron-withdrawing ability, the emission spectra of compound **1b**–**1f** are correspondingly bathochromically shifted to $\lambda = 486$, 491, 496, 497, and 508 nm, respectively, which might be attributed to the formation of a D-π-A system and consequent intramolecular charge transfer (ICT). To further confirm the presence of a charge-transfer state, the absorption and fluorescence spectra of compound **1e** were also performed in organic solvents with increasing polarity, as shown in Figure 4. On changing the solvent from toluene ($\varepsilon = 2.4$) to chloroform ($\varepsilon = 4.8$), THF ($\varepsilon = 7.5$), or DMF ($\varepsilon = 109.5$), no significant spectral change was observed in the UV/Vis spectra of **1e**. In comparison, the emission spectra are obviously redshifted from $\lambda = 491$ to 492, 498, or 517 nm. This hints at an ICT process in the excited state.[20] The quantum yields of compounds **1a**–**1f** in diluted methylene chloride were calculated to be 0.13, 0.14, 0.32, 0.27, 0.32, 0.25, respectively, by using 9,10-diphenylanthracene ($\Phi_f = 0.95$ in ethanol) as a standard.[48] Taking the single-crystal analysis and spectra characterization into consideration, we believe that different substituents are not only effective in preventing an oxidation reaction but also affect the optical properties to a great extent.

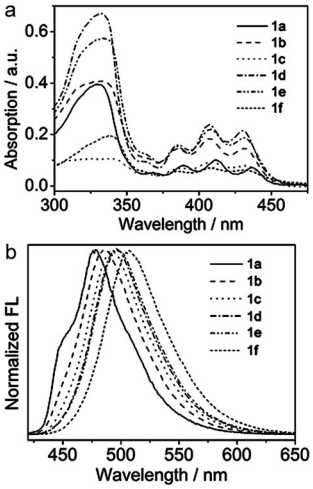

Figure 3. a) UV/Vis absorption spectra and b) normalized fluorescence spectra of compounds **1a**–**1f**. All spectra were measured in CH_2Cl_2 at 30 μM.

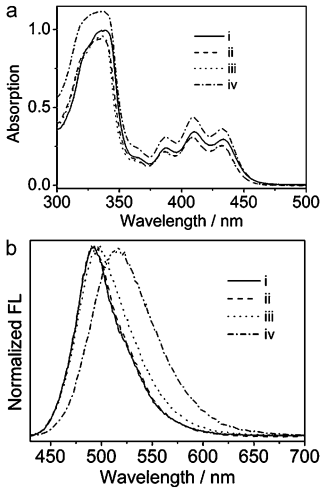

Figure 4. a) UV/Vis absorption spectra and b) normalized fluorescence spectra of compound **1e** in different solvents: i) toluene, ii) chloroform, iii) THF, iv) DMF.

To probe the redox properties of these compounds, cyclic voltammograms were measured by using 0.1 M tetrabutylammonium hexafluorophosphate (Bu_4NPF_6) as the supporting electrolyte according to the reported method.[16] The results are presented in Figure 5 and the detailed voltammetry data are compiled in Table S2 in the Supporting Information. In

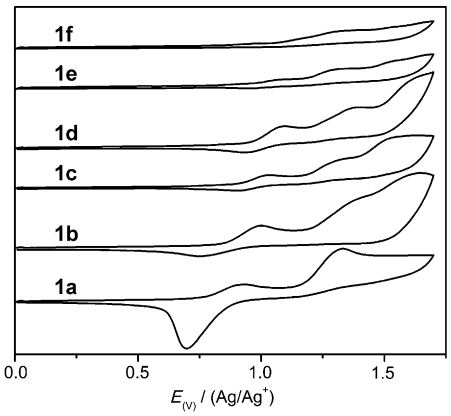

Figure 5. Cyclic voltammograms of **1a**–**1f** in anhydrous methylene chloride.

dry methylene chloride, compound **1a** shows the first reversible oxidative wave at 0.77 V and the second quasi-reversible oxidative wave at 1.14 V. In comparison, aryl-substituted compounds **1b–1f** also present two oxidative waves. However, the first oxidative waves were more positive at about 70, 130, 190, 40, and 50 mV, respectively, which indicates the relatively weaker oxidation ability. In addition, the band gaps of as-prepared **1a–1f** were estimated to be 2.76, 2.76, 2.74, 2.75, 2.75, and 2.70 eV on the basis of UV/Vis absorption data. Accordingly, the LUMO energy levels were calculated to be −2.41, −2.38, −2.56, −2.61, −2.46, and −2.52 eV. These cyclic voltammetry (CV) data is comparable to some sulfur-decorated acene derivatives, including five-membered rings.[28,52]

The 3D topology structures based on the crystal data of compounds **1a–1c** prompted us to study the inversion behavior from boat configuration to planar structure and then to chair configuration. To investigate the stability of this conformation, particularly in solution, a theoretical calculation was performed. Herein, the structure of **1b**, in which R = phenyl, was selected as the target molecule. The results reveal that dependent on the initial structure, the geometry optimization gives two possible results, chair and boat conformation, which correspond to the two benzene units bent to opposite sides or the same side, respectively. Interestingly, for both the chair and boat conformers, the absolute value of dihedral angles as indicated in Figure 6 are identical at

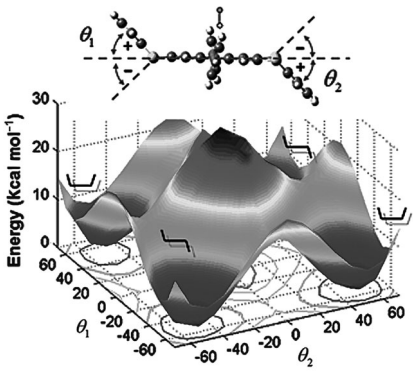

Figure 6. Two-dimension amplitude of the potential barrier as a function of the bend angles between benzene and the central planar skeleton.

52°, and the chair conformer has a single-point energy that is somewhat higher (1.7 kcal mol^{-1}) than that of the boat structure. Note that the difference in the dihedral value between the optimization and the crystal data (180–134.9 = 45°) should be ascribed to the intermolecular interaction in condensed phase, in which molecules tend to perform a further bending relative to their free state. Furthermore, to get the potential barrier between the both conformations, a scan calculation was made by individually altering the two dihedral angles from −70 to +70° in 10° increments. The results are depicted as a two-dimensional profile (Figure 6), in which the x and y axes are assigned to θ_1 and θ_2, respectively, and the z axis shows the relative energy of the conformer. As expected, the maximal potential (28 kcal mol^{-1}) occurs at the point of $\theta_1 = \theta_2 = 0°$, which corresponds to a planar structure. In addition, we found that when one of the terminal benzene moiety was kept at a fixed angle of 52° and the other was rotated, it was possible to reach the minimal barrier (14.3 kcal mol^{-1}) for the conformation transfer. Under these conditions, the potential energy can be plotted as a function of the single dihedral angle and additionally according to the energy level a Boltzmann distribution at 25 °C can be obtained (see Figure S1 in the Supporting Information).[60] In agreement with the crystal measurements, 80 % of free molecules take the chair conformation at 25 °C, and in comparison the population of the boat conformer is less than 5 %. However, there is a possible photoinduced conformation transfer because the minimal barrier is only 14.3 kcal mol^{-1}, which corresponds to a wavenumber of 5018 cm^{-1}.[61] Note that the geometry optimization and single-point energy calculation were all conducted at the B3LYP/6-31G level by using the Gaussian 09 package.[62]

To make a deep insight into the relationship of conformation and properties, the frontier molecular orbits obtained from the geometric optimization calculation are given in Figure 7 and Figure S2 in the Supporting Information. At

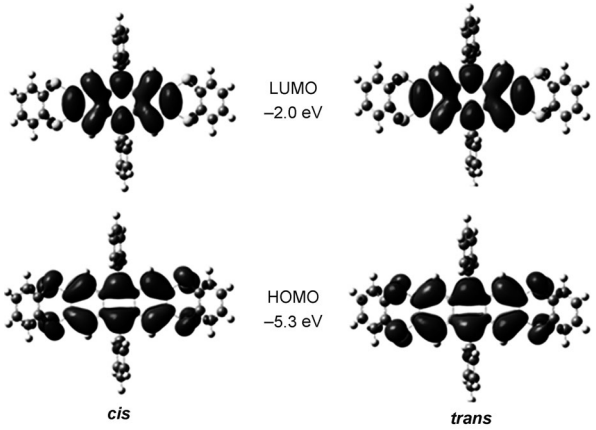

Figure 7. Comparison of the frontier orbitals of the *cis* and *trans* conformations of **1b**.

first glance, the orbital profiles are mainly distributed across the central planar skeleton, whereas the bent benzene units and vertical phenyl moieties make little or no contribution to the frontier orbital formation. Therefore, the similar spectral properties observed above for all compounds can be explained by the small effect of peripheral groups on the central chromophore. Based on this view, the similarity of the profile and energy level for the *cis* and *trans* conformers is easily understood because they all arise from the identical central chromophore. Clearly, the difference between the HOMO and LUMO is related to the lowest electric transition, which is in good agreement with the experimentally observed band in Figure 3 around $\lambda = 410$ nm (= 3.0 eV). It

is worth noting that the central planar skeleton consists of a basic structure of anthracene, which has been widely applied in highly efficient blue-light-emitting organic materials in energy-upconversion systems.[63,64] However, the crystal analysis reveals that these molecules prefer the chair conformation, which results in a more stable stack model than the boat conformation does; see, for example, the tube structure in **1e-ox**. Moreover, the properties of the frontier orbitals for all compounds investigated have been calculated and, as expected, no significant discrepancy has been observed for these molecules.

With these compounds in hand, the photoswitching behavior was measured to examine the photoinduced electron-transfer processes of heteroacenes **1a–1f** (donors), which were dropped onto a semiconducting single-walled carbon nanotube (sc-SWCNT, acceptor) thin film. As shown in Figure 8i (dashed line), a decreased photocurrent was produced

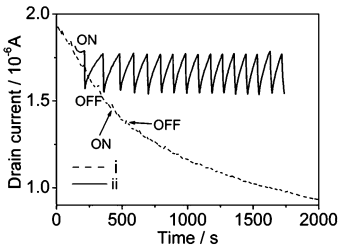

Figure 8. Photocurrent responses of i) sc-SWCNTs and ii) compound **1e**-sc-SWCNTs thin films at gate voltage (V_g) = −0.2 V and drain-source voltage (V_{ds}) = 2 V.

when the SWCNT film was irradiated by using a halogen lamp with an excitation level of 14.4 mW cm^{-2}, which might be ascribed to the photodesorption of oxygen in the devices. In contrast, under the same light irradiation at 2 V bias, a photocurrent response of 0.31 μA cm^{-2} for **1e**–SWCNT was produced (Figure 8ii, solid line). Additionally, the fall (turn on) and rise times (turn off) were found to be about 8 and 180 s, respectively. When **1a**, **1c**, **1d**, and **1f** were dispersed on SWCNT, obvious photocurrents were also observed as shown in Figure S3 in the Supporting Information. These results indicate that these heteroacenes could bond tightly to the SWCNT surfaces, which is beneficial for electron transfer. However, no photocurrent was generated for **1b**–SWCNT under the same conditions. Clearly, one can note that the response to the off cycle is hysteretic compared with the on cycle, which implies a typical trap-releasing current that is observed in some photocurrent-response devices.[54–56] In addition, the relative photocurrent change and the response speed of the donor–acceptor system showed negligible changes within the monitor time, which confirms that the as-prepared devices show good photosensitivity and stability.

Conclusion

A family of tetrathiaheptacene derivatives (**1a–1f**) was successfully synthesized and characterized. X-ray crystallography structure analysis showed that the as-prepared single crystals of **1a–1c** featured chair conformation, instead of planar or boat conformations, with dihedral angles between the anthracene unit and the terminal phenyl moieties of 137.258° for **1a**, 137.855° for **1b**, and 134.912°, which are close to the theoretical calculation results (≈128°). Based on the spectral analysis, one can note that the different substituents have a small effect on the UV/Vis spectra, but a significant effect on their emission wavelength owing to the ICT. Moreover, the HOMO–LUMO gaps of compounds **1a–1f** estimated from UV/Vis absorption and CV experiments correlated well with those obtained from DFT results. Compounds **1a–1f** were employed as the active layer in photoswitching devices that exhibited obvious photocurrent responses. Our systematic study may open new avenues for heteroacene molecular functionalization and further device preparation.

Acknowledgements

This work was supported by the National Natural Science Foundation of China (21102031, 21274037, and 91233107), the Ph.D. Programs Foundation of the Ministry of Education of China (20101301120004), the Natural Science Foundation of Hebei Province (B2014201007), and the Introduction of Overseas Students Funding of Hebei Province.

[1] A. Ajayaghosh, V. K. Praveen, *Acc. Chem. Res.* **2007**, *40*, 644.
[2] J. Wang, J. Yan, Z. Tang, Q. Xiao, Y. Ma, J. Pei, *J. Am. Chem. Soc.* **2008**, *130*, 9952.
[3] M. Bendikov, F. Wudl, D. F. Perepichka, *Chem. Rev.* **2004**, *104*, 4891.
[4] Y. Guo, Q. Tang, H. Liu, Y. Zhang, Y. Li, W. Hu, S. Wang, D. Zhu, *J. Am. Chem. Soc.* **2008**, *130*, 9198.
[5] S. Xiao, S. J. Kang, Y. Wu, S. Ahn, J. B. Kim, Y. L. Loo, T. Siegrist, M. L. Steigerwald, H. Li, C. Nuckolls, *Chem. Sci.* **2013**, *4*, 2018.
[6] J. Xiao, Z. Yin, H. Li, Q. Zhang, F. Boey, H. Zhang, Q. Zhang, *J. Am. Chem. Soc.* **2010**, *132*, 6926.
[7] H. Li, S. Kim, G. Ren, E. C. Hollenbeck, S. Subramaniyan, S. A. Jenekhe, *Angew. Chem. Int. Ed.* **2013**, *52*, 5513; *Angew. Chem.* **2013**, *125*, 5623.
[8] C. Fan, A. P. Zoombelt, H. Jiang, W. Fu, W. Yuan, Y. Wang, H. Li, H. Chen, Z. Bao, *Adv. Mater.* **2013**, *25*, 5762.
[9] S. Allard, M. Forster, B. Souharce, H. Thiem, U. Scherf, *Angew. Chem. Int. Ed.* **2008**, *47*, 4070; *Angew. Chem.* **2008**, *120*, 4138.
[10] T. Qin, G. Zhou, H. Scheiber, R. E. Bauer, M. Baumgarten, C. E. Anson, E. J. W. List, K. Müllen, *Angew. Chem. Int. Ed.* **2008**, *47*, 8292; *Angew. Chem.* **2008**, *120*, 8416.
[11] X. Hang, T. Fleetham, E. Turner, J. Brooks, J. Li, *Angew. Chem. Int. Ed.* **2013**, *52*, 6753; *Angew. Chem.* **2013**, *125*, 6885.
[12] T. Qin, W. Wiedemair, S. Nau, R. Trattnig, S. Sax, S. Winkler, A. Vollmer, N. Koch, M. Baumgarten, E. J. W. List, K. Müllen, *J. Am. Chem. Soc.* **2011**, *133*, 1301.
[13] J. Xiao, H. Yang, Z. Yin, J. Guo, F. Boey, H. Zhang, Q. Zhang, *J. Mater. Chem.* **2011**, *21*, 1423.
[14] J. Xiao, B. Yang, J. I. Wong, Y. Liu, F. Wei, K. J. Tan, X. Teng, Y. Wu, L. Huang, C. Kloc, F. Boey, J. Ma, H. Zhang, H. Yang, Q. Zhang, *Org. Lett.* **2011**, *13*, 3004.
[15] Y. Hong, J. W. Y. Lam, B. Tang, *Chem. Soc. Rev.* **2011**, *40*, 5361.

[16] Z. Liu, J. Xiao, Q. Fu, H. Feng, X. Zhang, T. Ren, S. Wang, D. Ma, X. Wang, H. Chen, *ACS Appl. Mater. Interfaces* **2013**, *5*, 11136.
[17] Y. Li, *Acc. Chem. Res.* **2012**, *45*, 723.
[18] C. Liu, S. Xiao, X. Shu, Y. Li, L. Xu, T. Liu, Y. Yu, L. Zhang, H. Liu, Y. Li, *ACS Appl. Mater. Interfaces* **2012**, *4*, 1065.
[19] L. Feng, C. Zhu, H. Yuan, L. Liu, F. Lv, S. Wang, *Chem. Soc. Rev.* **2013**, *42*, 6620.
[20] Y. Wang, J. Xiao, S. Wang, B. Yang, X. Ba, *Supramol. Chem.* **2010**, *22*, 380.
[21] D. Ding, K. Li, B. Liu, B. Tang, *Acc. Chem. Res.* **2013**, *46*, 2441.
[22] Y. Wu, Z. Yin, J. Xiao, Y. Liu, F. Wei, K. J. Tan, C. Kloc, L. Huang, Q. Yan, F. Hu, H. Zhang, Q. Zhang, *ACS Appl. Mater. Interfaces* **2012**, *4*, 1883.
[23] E. Clar, *Polycyclic Hydrocarbons*, Academic Press, London, **1964**.
[24] S. Kivelson, O. L. Chapman, *Phys. Rev. B* **1983**, *28*, 7236.
[25] K. N. Houk, P. S. Lee, M. Nendel, *J. Org. Chem.* **2001**, *66*, 5517.
[26] M. Bendikov, H. M. Duong, K. Starkey, K. N. Houk, E. A. Carter, F. Wudl, *J. Am. Chem. Soc.* **2004**, *126*, 7416.
[27] S. S. Zade, N. Zamoshchik, A. R. Reddy, G. Fridman-Marueli, D. Sheberla, M. Bendikov, *J. Am. Chem. Soc.* **2011**, *133*, 10803.
[28] J. E. Anthony, *Chem. Rev.* **2006**, *106*, 5028.
[29] M. Watanabe, Y. J. Chang, S. W. Liu, T. H. Chao, K. Goto, M. M. Islam, C. H. Yuan, Y. T. Tao, T. Shinmyozu, T. J. Chow, *Nat. Chem.* **2012**, *4*, 574.
[30] J. Li, Q. Zhang, *Synlett* **2013**, *24*, 686.
[31] D. Chun, Y. Cheng, F. Wudl, *Angew. Chem. Int. Ed.* **2008**, *47*, 8380; *Angew. Chem.* **2008**, *120*, 8508.
[32] I. Kaur, M. Jazdzyk, N. N. Stein, P. Prusevich, G. P. Miller, *J. Am. Chem. Soc.* **2010**, *132*, 1261.
[33] J. Xiao, H. M. Duong, Y. Liu, W. Shi, L. Ji, G. Li, S. Li, X. Liu, J. Ma, F. Wudl, Q. Zhang, *Angew. Chem. Int. Ed.* **2012**, *51*, 6094; *Angew. Chem.* **2012**, *124*, 6198.
[34] B. Purushothaman, M. Bruzek, S. R. Parkin, A. F. Miller, J. E. Anthony, *Angew. Chem. Int. Ed.* **2011**, *50*, 7013; *Angew. Chem.* **2011**, *123*, 7151.
[35] Q. Miao, T. Q. Nguyen, T. Someya, G. B. Blanchet, C. Nuckolls, *J. Am. Chem. Soc.* **2003**, *125*, 10284.
[36] C. Wang, J. Wang, P. Li, J. Gao, S. Y. Yan, W. Xiong, B. Hu, P. S. Lee, Y. Zhao, *Chem. Asian J.* **2014**, *9*, 779.
[37] D. Liu, X. Xu, Y. Su, Z. He, J. Xu, Q. Miao, *Angew. Chem. Int. Ed.* **2013**, *52*, 6222; *Angew. Chem.* **2013**, *125*, 6342.
[38] P. Gu, F. Zhou, J. Gao, G. Li, C. Wang, Q. Xu, Q. Zhang, J. Lu, *J. Am. Chem. Soc.* **2013**, *135*, 14086.
[39] U. H. F. Bunz, J. U. Engelhart, B. D. Lindner, M. Schaffroth, *Angew. Chem. Int. Ed.* **2013**, *52*, 3810; *Angew. Chem.* **2013**, *125*, 3898.
[40] G. Li, Y. Wu, J. Gao, J. Li, Y. Zhao, Q. Zhang, *Chem. Asian J.* **2013**, *8*, 1574.
[41] J. Li, J. Gao, G. Li, W. Xiong, Q. Zhang, *J. Org. Chem.* **2013**, *78*, 12760.
[42] G. Li, K. Zhang, C. Wang, K. S. Leck, F. Hu, X. Sun, Q. Zhang, *ACS Appl. Mater. Interfaces* **2013**, *5*, 6458.
[43] G. Li, Y. Wu, J. Gao, C. Wang, J. Li, H. Zhang, Y. Zhao, Q. Zhang, *J. Am. Chem. Soc.* **2012**, *134*, 20298.
[44] G. Li, H. M. Duong, Z. Zhang, J. Xiao, L. Liu, Y. Zhao, H. Zhang, F. Huo, S. Li, J. Ma, F. Wudl, Q. Zhang, *Chem. Commun.* **2012**, *48*, 5974.
[45] C. Dou, S. Saito, K. Matsuo, I. Hisaki, S. Yamaguchi, *Angew. Chem. Int. Ed.* **2012**, *51*, 12206; *Angew. Chem.* **2012**, *124*, 12372.
[46] B. D. Lindner, J. U. Engelhart, M. Märken, O. Tverskoy, A. L. Appleton, F. Rominger, K. I. Hardcastle, M. Enders, U. H. F. Bunz, *Chem. Eur. J.* **2012**, *18*, 4627.
[47] D. Li, H. Zhang, Y. Wang, *Chem. Soc. Rev.* **2013**, *42*, 8416.
[48] J. Xiao, X. Xiao, Y. Zhao, B. Wu, Z. Liu, X. Zhang, S. Wang, X. Zhao, L. Liu, L. Jiang, *Nanoscale* **2013**, *5*, 5420.
[49] J. Li, J. Gao, G. Li, W. Xiong, Q. Zhang, *J. Org. Chem.* **2013**, *78*, 12760.
[50] W. Jiang, Y. Li, Z. Wang, *Chem. Soc. Rev.* **2013**, *42*, 6113.
[51] C. Wetzel, A. Mishra, E. Mena-Osteritz, A. Liess, M. Stolte, F. Würthner, P. Bäuerle, *Org. Lett.* **2014**, *16*, 362.
[52] T. Mori, T. Nishimura, T. Yamamoto, I. Doi, E. Miyazaki, I. Osaka, K. Takimiya, *J. Am. Chem. Soc.* **2013**, *135*, 13900.
[53] K. Radhakrishnan, C. H. Lin, *Synlett* **2005**, 2179.
[54] R. Goossens, M. Smet, W. Dehaen, *Tetrahedron Lett.* **2002**, *43*, 6605.
[55] V. Coropceanu, J. Cornil, D. A. da Silva Filho, Y. Olivier, R. Silbey, J. L. Brédas, *Chem. Rev.* **2007**, *107*, 926.
[56] R. Qiao, A. P. Roberts, A. S. Mount, S. J. Klaine, P. C. Ke, *Nano Lett.* **2007**, *7*, 614.
[57] J. Xiao, S. Liu, Y. Liu, L. Ji, X. Liu, H. Zhang, X. Sun, Q. Zhang, *Chem. Asian J.* **2012**, *7*, 561.
[58] J. Xiao, C. D. Malliakas, Y. Liu, F. Zhou, G. Li, H. Su, M. G. Kanatzidis, F. Wudl, Q. Zhang, *Chem. Asian J.* **2012**, *7*, 672.
[59] J. Xiao, Y. Divayana, Q. Zhang, H. M. Doung, H. Zhang, F. Boey, X. Sun, F. Wudl, *J. Mater. Chem.* **2010**, *20*, 8167.
[60] A. Shimizu, T. Mori, Y. Inoue, S. Yamada, *J. Phys. Chem. A* **2009**, *113*, 8754.
[61] L. DeWitt, G. L. Blanchard, E. LeGoff, M. E. Benz, J. H. Liao, M. G. Kanatzidis, *J. Am. Chem. Soc.* **1993**, *115*, 12158.
[62] Gaussian 09, M. J. Frisch, G. W. Trucks, H. B. Schlegel, G. E. Scuseria, M. A. Robb, J. R. Cheeseman, G. Scalmani, V. Barone, B. Mennucci, G. A. Petersson, H. Nakatsuji, M. Caricato, X. Li, H. P. Hratchian, A. F. Izmaylov, J. Bloino, G. Zheng, J. L. Sonnenberg, M. Hada, M. Ehara, K. Toyota, R. Fukuda, J. Hasegawa, M. Ishida, T. Nakajima, Y. Honda, O. Kitao, H. Nakai, T. Vreven, J. A. Montgomery, Jr., J. E. Peralta, F. Ogliaro, M. Bearpark, J. J. Heyd, E. Brothers, K. N. Kudin, V. N. Staroverov, R. Kobayashi, J. Normand, K. Raghavachari, A. Rendell, J. C. Burant, S. S. Iyengar, J. Tomasi, M. Cossi, N. Rega, J. M. Millam, M. Klene, J. E. Knox, J. B. Cross, V. Bakken, C. Adamo, J. Jaramillo, R. Gomperts, R. E. Stratmann, O. Yazyev, A. J. Austin, R. Cammi, C. Pomelli, J. W. Ochterski, R. L. Martin, K. Morokuma, V. G. Zakrzewski, G. A. Voth, P. Salvador, J. J. Dannenberg, S. Dapprich, A. D. Daniels, Ö. Farkas, J. B. Foresman, J. V. Ortiz, J. Cioslowski, D. J. Fox, Gaussian, Inc., Wallingford CT, **2009**.
[63] P. I. Shih, C. Y. Chuang, C. H. Chien, E. W. G. Diau, C. F. Shu, *Adv. Funct. Mater.* **2007**, *17*, 3141.
[64] H. C. Chen, C. Y. Hung, K. H. Wang, H. L. Chen, W. S. Fann, F. C. Chien, P. Chen, T. J. Chow, C. P. Hsu, S. S. Sun, *Chem. Commun.* **2009**, 4064.
[65] R. R. Islangulov, J. Lott, C. Weder, F. N. Castellano, *J. Am. Chem. Soc.* **2007**, *129*, 12652.
[66] C. Soci, D. Moses, Q. H. Xu, A. J. Heeger, *Phys. Rev. B* **2005**, *72*, 245204.
[67] J. Xiao, Z. Yin, B. Yang, Y. Liu, L. Ji, J. Guo, L. Huang, X. Liu, Q. Yan, H. Zhang, Q. Zhang, *Nanoscale* **2011**, *3*, 4720.
[68] Y. Liu, N. Wang, Y. Li, H. Liu, Y. Li, J. Xiao, X. Xu, C. Huang, S. Cui, D. Zhu, *Macromolecules* **2005**, *38*, 4880.

Received: March 17, 2014
Published online: ■■ ▮▮, 0000

FULL PAPER

Heteroacenes

Tiejun Ren, Jinchong Xiao, Wenying Wang, Wenya Xu, Sujuan Wang, Xuemin Zhang, Xuefei Wang,* Hua Chen,* Jianwen Zhao,* Li Jiang* ____–____

Synthesis, Crystal Structures, Optical Properties, and Photocurrent Response of Heteroacene Derivatives

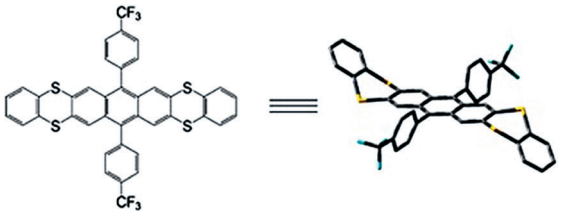

Pull up a chair! Six 5,9,14,18-tetrathiaheptacene derivatives (**1a**–**1f**) were synthesized and characterized (see figure). Derivatives **1a**, **1b**, and **1c** adopt a chair conformation and the dihedral angle between anthracene and the terminal benzene units were 137.258, 137.855, and 134.912°, respectively. Moreover, the photoswitching behavior with **1a**–**1f** as donors and SWCNT as an acceptor indicated that these heteroacenes are promising organic semiconductor materials.